duction band edge for the carbon sites. In addition to the electronic structure information, we were able to determine the F-C bond length to be 1.38 Å and we also found indications that structural ordering holds strongly through the tertiary neighbors to fluorine.

Acknowledgments. This work was performed at the Stanford Synchrotron Radiation Laboratory, which is supported by the NSF Grant 77-27489, in cooperation with the Stanford Linear Accelerator Center and was done with support from the Division of Chemical Sciences, Office of Basic Energy Sciences, U.S. Department of Energy, under Contract W-7405-Eng-48. The authors wish to thank Peter Young, Gustav Apai, and Paul Wehner for their contributions to the early stages of this work, Wini Heppler for making the thin films used in this study, and Joseph Katz and Richard Strudwick for designing and building the electronics that made the experiment possible.

Rotational Motions of Side Chains of Poly-L-lysine

Richard J. Wittebort, Attila Szabo, and Frank R. N. Gurd*

Contribution from the Department of Chemistry, Indiana University, Bloomington, Indiana 47405. *Received March 10, 1980*

Abstract: The ^{13}C NMR relaxation times and nuclear Overhauser enhancements have been measured for the protonated carbons of poly-L-lysine at 15.1 and 67.9 MHz. To characterize the structure of the polylysine we have examined both the CD and ^{13}C NMR spectra at 3 and 28 °C at pH values between 10 and 11 in the neighborhood of the helix-coil transition. At 3 and 28 °C for pH values above the completion of the random coil-helix transition the peptide readily aggregates at the concentrations used. Consequently, to avoid the aggregation, we have studied the NMR relaxation under the conditions 3 °C and pH 10.7, where the poly-L-lysine does not have a rigidly structured α-helical backbone. The relaxation data are interpreted in terms of a recently developed theoretical formalism. The simplest model for the molecular motions consistent with the frequency-dependent NMR data assumes that backbone carbons, C^{α}, are characterized by a distribution of correlation times, or diffusion constants as used here, and the side-chain carbons, C^{β}, C^{γ}, C^{δ}, and C^{ϵ}, undergo independent axial motions with *restricted* angular amplitudes.

High-resolution nuclear magnetic relaxation studies can, at least in principle, give detailed information about rotational dynamics of molecules in solution. This is because the relatively low, i.e., radio, absorption frequency of NMR experiments conveniently coincides with the characteristic frequencies of molecular rotational motions in condensed phases. In this study we apply a recently developed theoretical formalism[1,2] to extract detailed motional information from the ^{13}C longitudinal relaxation times and nuclear Overhauser enhancements of the protonated carbons in poly-L-lysine.

A similar study of poly(*n*-alkyl methacrylates) has been reported by Levy et al.[3] These authors attempted to describe their relaxation data in terms of a generalization of a model proposed originally by Wallach.[4] The side-chain *n*-alkyl carbons are assumed to be undergoing consecutive independent and free axial diffusion-like motions about the C-C bonds. The side-chain motion is superimposed on isotropic backbone motion which, as suggested by Schaefer,[5] is characterized by a distribution of correlation times or rotational diffusion constants. These authors found that the frequency-dependent relaxation data of the side-chain carbons is not consistent with this description.

One expects that the assumption of free axial motions about the side-chain C-C bonds is unrealistic in that the allowed conformational space is too large. The Wallach model has recently been generalized by Wittebort and Szabo[1] to incorporate excluded volume effects by restricting the *amplitude* of internal rotations and, independently, by London and Avitabile[2] for the case of a single internal rotation. In this study we further extend the model to allow the α carbon to possess a distribution of rotational correlation times. In order to make this model computationally feasible, a distribution function for the backbone diffusion constants was chosen such that the required averages of the spectral density functions could be performed analytically rather than numerically as has been done previously for the Wallach model.[3]

Materials and Methods

The polylysine used in this study was prepared by Miles-Yeda Ltd. and obtained from Miles Laboratories, Elkhart, Ind. The material, Code 71-120, Lot 250, and molecular weight 27 000, had a degree of polymerization of 129.

Polylysine samples in 0.1 M NaF were prepared by dissolving 660 mg of the HBr salt in 12 mL of deionized and distilled H_2O. The solution was titrated to pH 10.6 by the addition of redistilled HCl at 3 °C, and then dialyzed overnight against H_2O. Subsequently, the volume was decreased to the original 12 mL and sufficient NaF was added to be 0.1 M in this salt. The pH was adjusted to the desired value at 25 or 3 °C prior to the NMR experiment.

^{13}C NMR spectra were obtained on home-built spectrometers operating at either 15.01 or 67.9 MHz. The 90° H_1 pulse widths on the two spectrometers were typically 37 μs (15.1 MHz spectrometer) or 18.5 μs (67.9 MHz spectrometer) and were redetermined prior to each relaxation study. Relaxation studies were done by using the inversion recovery method, i.e., 180°-τ-90° pulse sequences. T_1 values were determined from the inversion recovery experiments by fitting the intensities, $I(\tau)$, of each NMR line to the function $I(\tau) = A + Be^{-T_1/\tau}$, using a nonlinear least-squares fitting program, BMDX85.[6,7]

Nuclear Overhauser enhancements, NOE's, were measured at 67.9 MHz, using the gated decoupling method with 100-Hz square-wave modulation and a recycle time of 4.0 s. Error analysis of the NOE values was carried out by calculating the standard deviation, σ, in the integrated intensities, I_G, of the protonated carbon resonances in the spectrum obtained with gated decoupling. Since all resonances in this spectrum should have the same intensity, σ is a measure of the uncertainty in these values. The uncertainties for the NOE values were calculated from the relation $NOE_{\pm} = (I_{cw} \pm \sigma)/(I_G \mp \sigma)$ where NOE_+ and NOE_- are taken

(1) Wittebort, R. J.; Szabo, A. *J. Chem. Phys.* **1978**, *69*, 1722.
(2) London, R. E.; Avitabile, J. *J. Am. Chem. Soc.* **1978**, *100*, 7159.
(3) Levy, G. C.; Axelson, D. E.; Schwartz, R.; Hockmann, J. *J. Am. Chem. Soc.* **1978**, *100*, 410.
(4) Wallach, D. *J. Chem. Phys.* **1967**, *47*, 5258.
(5) Schaefer, J. A. *Macromolecules* **1973**, *6*, 882.
(6) Kowalewski, J.; Levy, G. C.; Johnson, L. F.; Palmer, L. *J. Magn. Reson.* **1977**, *26*, 533.
(7) Dixon, W. J., Ed., 1965, BMD Biomedical Computer Programs, University of California Press: Los Angeles, BMDX85, April, 1971, revision, developed at the Health Sciences Computing Facility, UCLA, sponsored by NIH Special Research Resources Grant RR-3.

0002-7863/80/1502-5723$01.00/0 © 1980 American Chemical Society

as the upper and lower uncertainty limits, respectively.

Theory

The interpretation of magnetic relaxation experiments in polymers has proceeded along two lines. In the case of random high molecular weight materials such as polyethylene, Schaefer[5] assumed that the rotational motions executed by the polymer are characterized by a distribution of correlation times or diffusion constants. It is found that the range of diffusion constants can vary over several orders of magnitude.[3,5]

In the case of the four C–C segments of a lysyl amino acid side chain, the number of characteristic correlation times is greatly reduced. Consequently models for relaxation in short chains have concentrated on the rate (diffusion constant) and amplitude of the motion about the individual C–C segments.[1,2,4]

The experimental system of polylysine examined here can have elements of both the foregoing descriptions. An unstructured polypeptide backbone containing 129 peptide units is analogous to the case of polyethylene whereas the short lysyl side chain yields ^{13}C NMR resonances for each carbon atom and can be treated in terms of the motion about each C–C segment.

We thus construct a generalized model in which side-chain motion, described by the rate and amplitude of independent axial diffusion about each of the four C–C bonds, is superimposed on the isotropic rotational diffusion of the backbone. Furthermore, the backbone motion is characterized by a distribution of rotational diffusion constants.

The general formulas relating the longitudinal relaxation time, T_1, and the nuclear Overhauser enhancement, NOE, to spectral density functions have been summarized in ref 1. For the case of a single backbone diffusional constant, D, the general form of the spectral density, $J'(\omega)$, is a sum of lorentzians[1]

$$J'(\omega) = \sum_{a,b,\ldots} C_{a,b,\ldots}\left[\frac{6D + \lambda_{a,b,\ldots}}{(6D + \lambda_{a,b,\ldots})^2 + \omega^2}\right] \quad (1)$$

The explicit forms of $C_{a,b,\ldots,n}$ and $\lambda_{a,b,\ldots,n}$ which take into account the rates and amplitudes of each of the consecutive internal diffusion processes are given in the Appendix.

In the case at hand, eq 1 must be appropriately averaged over some distribution of D. Schaefer[5] chose the very wide asymmetric log $-\chi^2$ distribution which favors small values of D. For this distribution the integration must be performed numerically. The spectral density is not expected to be very sensitive to the precise form of the distribution. This is somewhat analogous to the situation which arises in the theory of specific heats of crystals.[8] The Debye approximation for the normal mode frequency distribution looks nothing like (except, of course, at low frequencies) the exact distribution, yet the resulting heat capacity is extremely accurate. For mathematical simplicity we assume a broad asymmetric distribution in which the probability of log D is constant over the interval from D_L to D_U. The normalized distribution function for D is then

$$p(D) = [\ln (D_U/D_L)D]^{-1} \quad (2)$$

Averaging eq 1 according to eq 2 yields the following analytic result for $J'(\omega)$:

$$J'(\omega) = (\ln D_U/D_L)^{-1} \int_{D_L}^{D_U} J'(\omega)\, d \ln D$$

$$J'(\omega) = \sum_{a,b,\ldots} C_{a,b,\ldots}[\ln (D_U/D_L)(\lambda^2_{a,b,\ldots} + \omega^2)]^{-1} \times \left[\omega \tan^{-1}\left(\frac{6(D_U - D_L)\omega}{\omega^2 + (6D_U + \lambda_{a,b,\ldots})(6D_L + \lambda_{a,b,\ldots})}\right) + \frac{\lambda_{a,b,\ldots}}{2} \ln\left(\frac{D_U^2((6D_L + \lambda_{a,b,\ldots})^2 + \omega^2)}{D_L^2((6D_U + \lambda_{a,b,\ldots})^2 + \omega^2)}\right)\right] \quad (3)$$

(8) Zemansky, M. W. "Heat and Thermodynamics", 5th ed.; McGraw-Hill: New York, 1968.

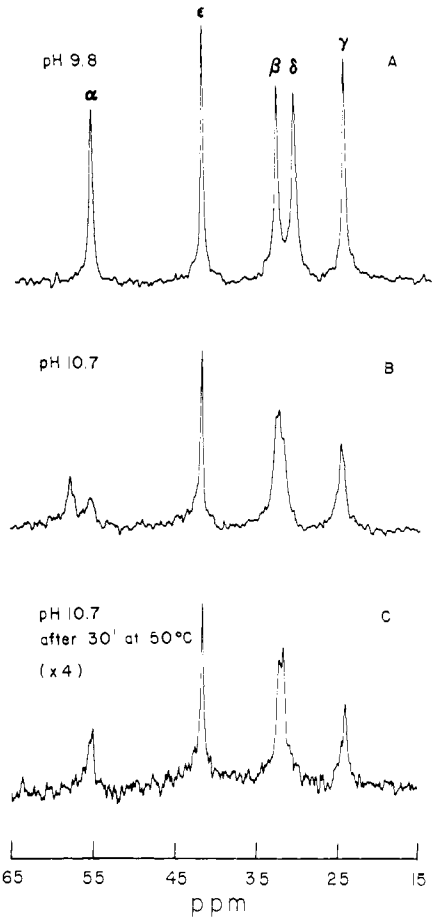

Figure 1. The pH dependence of 67.9-MHz ^{13}C NMR spectra of $(Lys)_{129}$ at 28 °C.

We note that for the case of no internal motion, e.g., for C^α, the spectral density has the following simple form:

$$J'(\omega) = [\omega \ln (D_U/D_L)]^{-1} \tan^{-1}\left[\frac{6(D_U - D_L)\omega}{\omega^2 + 36D_UD_L}\right] \quad (4)$$

Results

A. General Spectral Features. The structure of poly-L-lysine has been studied extensively by a variety of physical techniques[9-14] including circular dichroism, pH titration, ^1H NMR, and ^{13}C NMR. The primary finding is that in dilute solutions poly-L-lysine undergoes a random coil–helix transition upon deprotonation of the ε-amino group. We report here simultaneous NMR and circular dichroism spectra obtained from poly-L-lysine samples at 28 and 3 °C and over the pH range of the coil–helix transition.

Circular dichroism spectra obtained at room temperature and various pH values with the $(Lys)_{129}$ used in this study are in accord with previous findings.[9,10] As the pH value is raised above 10.5, there is little change in the spectrum, indicating completion of the coil–helix transition.

In Figure 1 are shown 67.9-MHz ^{13}C NMR spectra of 3.2% polylysine solutions obtained at 28 °C and pH values of (A) 9.8 and (B) 10.7, as well as an additional spectrum (C) at pH 10.7 after being subjected to 50 °C for 20 min. To facilitate comparison

(9) Holzwarth, G.; Doty, P *J. Am. Chem. Soc.* **1965**, *87*, 218.
(10) Nagasawa, M.; Holtzer, A. *J. Chem. Soc.* **1964**, *8*, 538.
(11) Fasman, G. D.; Lindblow, C.; and Bodenheimer, E. *Biochemistry* **1964**, *3*, 155.
(12) Saito, H.; and Smith, I. C. P. *Arch. Biochem. Biophys.* **1973**, *158*, 154.
(13) Appel, P.; Yang, J. T. *Biochemistry* **1975**, *4*, 1244.
(14) Bradbury, E. M.; Crane-Robinson, C.; Goldman, H.; Rattle, H. W. E. *Biopolymers* **1968**, *6*, 851.

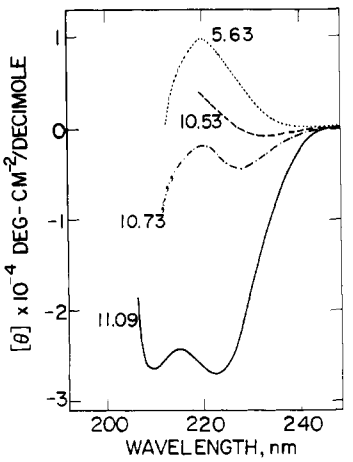

Figure 2. CD spectra of $(Lys)_{239}$ at 3 °C and various pH values: pH 11.09 (—), pH 10.73 (---), pH 10.53 (---), and pH 5.63 (. . .).

the vertical scales of the spectra were normalized in proportion to the number of accumulations, and subsequently the scale of spectrum C was multiplied by 4. The indicated resonance assignments are those of Keim et al.[15]

In raising the pH from 9.8 (Figure 1A) to 10.7 (Figure 1B), the resonances due to C^{α}, C^{β}, C^{δ}, and probably C^{γ} are doubled and indicate two sets of overlaid spectral components. All lysine ^{13}C resonances in simple peptides are known to titrate downfield with increasing pH.[15] Saito and Smith[12] observed that the titration behavior in the pH range from 6.5 to pH 11.5 for $(Lys)_{12}$, which does not form helices, is the same as for $(Lys)_{130}$. Thus it was concluded that the coil–helix transition has little effect on the ^{13}C chemical shifts. These authors further observed that the heat-induced formation of the β structure yields a clear downfield shift of the C^{α} resonance. The upfield component of the C^{α} resonance in Figure 1B is that expected from simple titration of the ϵ-amino group and thus corresponds to the α-helical structure, and the downfield component most likely corresponds to the β structure. Heating the sample for 20 min at 50 °C results in a nearly complete gelation of the previously nonviscous sample. The resulting spectrum, Figure 1C, was obtained only after more extensive signal averaging and shows single resonances. In particular, the C^{α} resonance corresponds to the resonance assigned to that for the α-helical conformation in Figure 1B. Also apparent in Figure 1C and not in Figures 1A or 1B is considerable bulging of the baseline between 25 and 55 ppm due to very broad resonances. It is thus likely that the heat treatment causes an intermolecular aggregation of the β structure yielding the highly viscous gel state and the observed very broad resonances, whereas the narrower resonances in Figure 1C correspond to residual α-helical structure. By comparison of the C^{α} resonances in Figures 1A and 1C, the C^{α} resonance in Figure 1C accounts for 10% of the polylysine concentration.

The simultaneous appearance of β- and α-helical structures observed above has also been reported in the literature. Bradbury et al.[14] suggest that the problem is overcome at lower peptide concentrations than used here by performing the experiments at temperatures below 5 °C.

Shown in Figure 2 are CD spectra of dilute solutions of $(Lys)_{129}$ at several pH values. The sample cell was thermostated at 3 °C. Immediately apparent is that high helical content is observed only for pH values greater than 11, as expected on the basis of the temperature-dependent increase of the ϵ-amino pK_a by about 0.6 unit.[16]

In Figure 3 are shown ^{13}C NMR spectra obtained from 3.2% solutions of polylysine at 3 °C. In passing from pH 10.5 (Figure 3A) to pH 10.7 (Figure 3B), the C^{α} resonance in particular broadens somewhat, but all resonances are symmetrical. With further raising of the pH to 10.9 (Figure 3C), the onset of doubled resonances is observed as before at room temperature. A twofold dilution of the sample used in Figure 3C gives the spectrum shown in Figure 3D and does not eliminate the doubled resonances.

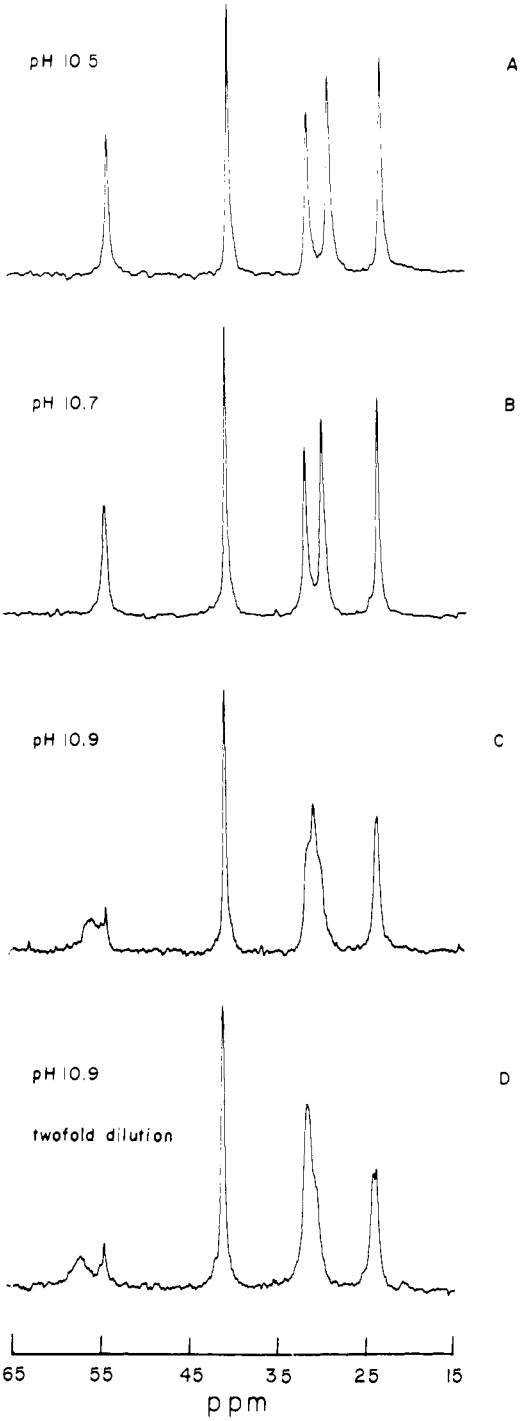

Figure 3. The pH and concentration dependence of 67.9-MHz ^{13}C NMR spectra of $(Lys)_{129}$ at 3 °C.

Table I. Measured NT_1 and NOE Values

carbon	67.9 MHz NT_1 (MS)	67.9 MHz NOE[a]	15.1 MHz NT_1 (MS)
C^{α}	170 ± 8	1.6 ± 0.2	36 ± 3
C^{β}	202 ± 8	2.0 ± 0.2	72 ± 11
C^{γ}	264 ± 12	2.4 ± 0.2	108 ± 11
C^{δ}	430 ± 20	2.3 ± 0.2	208 ± 23
C^{ϵ}	734 ± 50	2.7 ± 0.2	484 ± 69

[a] NOE is defined as $(1 + \eta)$.

(15) Keim, P.; Vigna, R. A.; Nigen, A. M.; Morrow, J. S.; Gurd, F. R. N. *J. Biol. Chem.* **1974**, *249*, 4149.

(16) Cohn, E. J.; Edsall, J. T. "Proteins, Amino Acids and Peptides as Ions and Dipolar Ions"; Reinhold: New York, 1943; 89.

Table II. Calculated Diffusion Constants and NOE and T_1 Values from Free Diffusion Model

carbon	calcd D_i from 67.9-MHz T_1 (10^9 s^{-1})	calcd D_i from 15.1-MHz T_1 (10^9 s^{-1})	67.9-MHz NOE theory[a] (expt)	67.9-MHz T_1 (MS) theory[b] (expt)	15.1-MHz T_1 (MS) theory[a] (expt)
C^β	1.2 ± 0.17	0.56 ± 0.10	2.68 (2.0 ± 0.2)	151 (202 ± 8)	188 (72 ± 11)
C^γ	1.2 ± 0.17	0.48 ± 0.11	2.68 (2.4 ± 0.2)	167 (264 ± 12)	207 (108 ± 11)
C^δ	2.1 ± 0.25	1.1 ± 0.02	2.87 (2.3 ± 0.2)	255 (430 ± 20)	394 (208 ± 23)
C^ϵ	3.3 ± 0.6	3.3 ± 0.6	2.95 (2.7 ± 0.2	520 (734 ± 50)	702 (484 ± 69)

[a] Calculated from D_i's determined from 67.9-MHz T_1 data. [b] Calculated from D_i's determined from 15.1-MHz T_1 data.

Table III. Calculated Amplitudes, Diffusion Constants, and NOE and T_1 Values from the Restricted Diffusion Model

carbon	$\pm\gamma_i$ (deg)	best fit D_i (10^9 s^{-1})	67.9-MHz NOE calcd (exptl)	67.9-MHz T_1 (MS) calcd (exptl)	15.1-MHz T_1 (MS) calcd (exptl)
C^β	±60	1.0	2.13 (2.0 ± 0.2)	205 (202 ± 8)	69 (72 ± 11)
C^γ	±50	1.5	2.40 (2.4 ± 0.2)	254 (264 ± 12)	117 (108 ± 11)
C^δ	±120	3.3	2.55 (2.3 ± 0.2)	409 (430 ± 20)	224 (208 ± 23)
C^ϵ		3.3	2.86 (2.7 ± 0.2)	680 (734 ± 50)	574 (484 ± 70)

Because of overlapping spectral components due to the presence of both α-helical and β structures at pH values near and above the coil–helix transition endpoint, we have chosen to investigate the ^{13}C NMR relaxation of poly-L-lysine at 3 °C and a pH value of 10.7. By CD criteria, the structure of the polypeptide is predominantly disordered under these conditions.

B. Relaxation Study. Shown in Figure 4 is a set of 67.9-MHz ^{13}C NMR inversion recovery spectra obtained with a 3.2% solution of $(Lys)_{129}$. The T_1 values determined from these spectra and from an equivalent experiment at 15.1 MHz are collected in Table I along with the 67.9-MHz NOE values.

First the results for C^α are discussed. For a rigidly structured polypeptide backbone of 129 residues the overall diffusional motion will be sufficiently slow that a minimum value of 1.153 for the NOE is expected.[17] The experimentally measured value of 1.6 ± 0.2 indicates, in agreement with the CD results, that the backbone is not rigid but relatively flexible. Assuming the motional model for C^α presented in the Theory section (eq 4), we find that the two parameters, i.e., D_L and D_U which are the lower and upper limits of the diffusional constant distribution, are uniquely determined by the two observed T_1 values for C^α. These parameters, $D_L = 2.5 \times 10^6$ s^{-1} and $D_U = 5.0 \times 10^8$ s^{-1}, reproduce the T_1 values exactly and consequently predict a 67.9-MHz NOE value of 1.6 in agreement with that observed in this work.

The relaxation data for the lysyl side chain carbons, i.e., C^β, C^γ, C^δ, and C^ϵ, given in Table I are now subjected to analysis by two types of models for consecutive internal reorientation. The first model, proposed initially by Wallach,[4] assumes that each of the internal motions is an independent, axial, diffusion process. For example, viewed from the δ carbon the $^{13}C^\epsilon$–^1H vector is seen as simply undergoing rotational diffusion about the C^δ–C^ϵ bond axis with diffusion constant D_ϵ. Similarly, the δ carbon is rotationally diffusing about the C^δ–C^γ bond axis with diffusion constant D_δ when viewed from the β carbon, and so on. Since in this model a rotation about, say, the C^β–C^γ bond not only reorients a C^γ–H vector but also the C^δ–H and C^ϵ–H vectors, we expect the diffusion constants to increase monotonically toward the end of the chain, i.e., $D_{\beta_1} < D_\gamma < D_\delta < D_\epsilon$.

As discussed previously the four diffusion constants are uniquely determined from the T_1 values for C^β, C^γ, C^δ, and C^ϵ observed at a single spectrometer frequency. With the values given above for D_L and D_U, D_β is varied (in eq A2a and A2b) to reproduce the T_1 for C^β. This value of D_β, along with D_L and D_U, is then used to determine D_γ from the T_1 for $C\gamma$, and so on. Aside from the possibility of satisfying the internal consistency argument, i.e., that $D_\beta < D_\gamma < D_\delta < D_\epsilon$, these computed parameters tell us nothing about the validity of the model. Of particular importance in this regard are additional observations such as NOE measurements and T_1 values determined at two spectrometer frequencies.

Shown in the first two columns of Table II are the diffusion constants for the lysyl side-chain carbons determined from the T_1 data obtained at 67.9 and 15.1 MHz. Immediately apparent is that the diffusion constants, with the exception of D_ϵ, are a factor of 2 greater when determined from the 67.9-MHz T_1 data as compared to those determined at 15.1 MHz. In column 3 of Table II the NOE values predicted on the basis of the diffusion constants determined from the 67.9-MHz T_1 data are compared with the experimental values. The theoretical values are systematically greater than those observed. Compared in the last two columns of Table II are high-field (67.9 MHz) T_1 values calculated by using the D_i's determined at the low-field (15.1 MHz), and vice versa. The low-field D_i's considerably underestimate the high-field T_1's and, conversely, the high-field D_i's overestimate the low-field T_u values. The disagreement is so great that the calculated 15.1-MHz T_1 values are noticeably larger than those calculated for the higher frequency. Thus the data show that this model is unreasonable as is to be expected from physical considerations.

An obvious difficulty with the free diffusion model is that by assuming free rotation about each of the bonds the allowed conformational space is much too large. Neglected in the Wallach model are the facts that the side-chain cannot crossover on itself or occupy the same volume as the peptide backbone. These excluded volume effects can be accounted for in a heuristic way by restricting the amplitudes of the internal rotations to occur within a specified angular region.[1,2] This has a pronounced effect

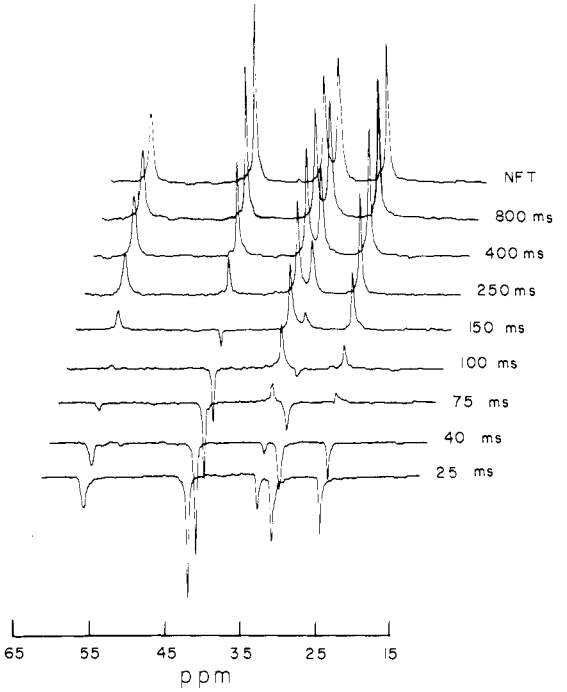

Figure 4. The 67.9-MHz inversion recovery set for $(Lys)_{129}$ obtained at 3 °C and pH 10.67. The delay time between 180° pulses was 3 s.

(17) Allerhand, A.; Oldfield, E. *Biochemistry* **1973**, *12*, 3428.

at lower frequencies such as 15.1 MHz of decreasing the T_1 value for a given diffusion constant.

The results of fitting the data to the restricted diffusion model are compiled in Table III. The method for determining the parameters is essentially the same as that for the previous case except that the three additional angular parameters, γ_i, are determined by attempting to find a unique pair of values for D_i and γ_i which simultaneously reproduce both the low- and high-frequency T_1 values for the corresponding carbon atom. It should be pointed out that the fits shown in Table III are not the best possible in the least-squares sense, and somewhat better agreement could have been obtained by further optimization.

Immediately apparent from Table III is that the relaxation times calculated from a single set of D_i and γ_i are in good agreement with the experimental values obtained at both spectrometer frequencies. In addition, the theoretical NOE values agree with those determined experimentally. Also the self-consistency requirement is nominally satisfied. The only poor fit, which is for C^ϵ, could likely be improved by also restricting the diffusion about the C^δ–C^ϵ bond. This is not physically unreasonable since motions about the C^δ–C^ϵ bond must reorient the bulky hydrated ammonium group.

Discussion

The simple two-parameter model presented here for the backbone motion is found to be consistent with the observed frequency dependence of the relaxation times and correctly predicts the NOE for C^α. We note that a calculation using a uniform distribution, $p(D) \propto$ constant, does not work. We now consider the magnitude of these diffusion constant limits and the range over which they vary.

The value $D_L = 2.5 \times 10^6\ s^{-1}$ is small compared to the effective rotational diffusion constant of $4 \times 10^7\ s^{-1}$ determined by Allerhand and Oldfield[17] for the compact helical form of poly(γ-benzyl glutamate) of similar molecular weight to that of the $(Lys)_{129}$ studied here. This comparison indicates the presence of slow motions likely corresponding to the reorientation of an extended or partially extended structure. The value $D_U = 5.0 \times 10^8\ s^{-1}$ calculated for the much less probable $(p(D_U)/p(D_L) = 5 \times 10^{-3})$ fast motion limit is still a factor of ~ 2 slower than the slowest of the side-chain motions, i.e., that for the rotation of a four-bond segment. Similarly, the mean value for this distribution, $(D_L D_U)^{1/2} \simeq 4 \times 10^7\ s^{-1}$, is two orders of magnitude slower than the side-chain diffusion.

Based on the assumed distribution, the C^α diffusion constants are calculated to vary over a range of more than two orders of magnitude. This range, wide compared to the one or two characteristic diffusion constants expected for a spherical or rod-like macromolecule, is still narrow compared to the ranges of three to five orders of magnitude estimated for materials such as polybutadiene or polystyrene. Schaefer[5] has interpreted the narrower range observed for solid polybutadiene relative to solid polyisoprene or dissolved polystyrene to indicate a predominance of long-range cooperative motions in the case of polybutadiene. The narrow distribution estimated for polylysine in this work similarly indicates a long-range type of motion. Such backbone motions likely arise as a consequence of the onset of helix formation expected on the basis of the CD results, shown in Figure 2. In other words, the sample is not completely random but partially helical.

We now consider the results from the side-chain calculations. At this point it is useful to note that the side-chain diffusion constants are relatively insensitive to the model assumed for the motion of C^α. For example, in the case of the free diffusion model essentially the same set of D_i's given in Table II are calculated from the data (Table I) if it is assumed that the backbone motion is isotropic with a single diffusion constant of $3.4 \times 10^7\ s^{-1}$.[18]

In this study two models are used to analyze the side-chain relaxation data. With the free diffusion model, the internal rotations about consecutive bonds are assumed to be free and independent axial diffusion processes. The free diffusion model accounts for neither the frequency dependence of the relaxation times nor the Overhauser enhancements. Similar conclusions have been reached by Levy et al. in a study of poly(*n*-alkyl methacrylates).[3] The restricted diffusion model, which does account for the data, is modified to allow for excluded volume effects. The independent reorientation about each bond is assumed to be diffusion within a square-well potential. The two phenomenological parameters D_i and $2\gamma_i$ give the rate of the diffusion and the width of the square well, respectively. The results of this study thus indicate that if one neglects the angular restriction and makes $2\gamma_i = 360°$ (essentially the free diffusion model), an effective value of D_i cannot be chosen to account for the frequency dependence of the T_1 values.

The angular amplitudes, $2\gamma_i$, of 120, 110, and 240° calculated for the rotations about the C^α–C^β, C^β–C^γ, and C^γ–C^δ bonds, respectively, correspond to possible total amplitudes for 120° jump-like motions among the well-known rotational isomers. More sophisticated and realistic models of nuclear relaxation based on jump motions have been proposed,[1] but their use for this experimental system seems unwarranted. The lack of a rigidly structured backbone makes the choice of a set of side-chain configurations arbitrary, and the possibility of chain motions coupling to the backbone motion suggests that the experimental system is too complex for a more sophisticated analysis to be meaningful.

It is of interest to compare the experimental and phenomenological constants determined in this study with those obtained from proteins. The T_1 of 484 ms measured for C^ϵ of polylysine is larger than the value of 278 as measured at the same frequency by Glushko et al.[19] for lysyl C^ϵ resonances in the small protein ribonuclease, indicating a reduced mobility of lysyl groups in the protein. In a recent study of myoglobin,[20] using the techniques described here, the diffusion constants for the methyl group rotation and terminal bond motion ($\gamma^\gamma \simeq 30$–$40°$) in isoleucine residues were in the neighborhood of 3×10^{10} and $1 \times 10^{10}\ s^{-1}$, respectively. The value of $1 \times 10^{10}\ s^{-1}$ is thus larger than the corresponding value of $D_\epsilon = 3.3 \times 10^9\ s^{-1}$ for a lysyl residue in either polylysine or ribonuclease. It thus seems likely that the motions of nonpolar side chains in the hydrophobic interior of a protein, although damped in amplitude by packing constraints, can be more rapid than that of hydrated polar groups exposed on the surface.

Finally we conclude that sufficiently extensive nuclear magnetic relaxation data can be interpreted to yield physically meaningful information about the rates and amplitudes of molecular motions. The Wallach model, which is clearly physically unreasonable, is indeed incapable of explaining the data. The model considered is the simplest which can explain the data. The qualitative picture which emerges from our analysis, namely, that as one goes out the side chain the angular restraint decreases while the rate of motion increases, is phycially satisfying.

Acknowledgments. This research was supported by U.S. Public Health Service Grants HL-05556 and HL-21483, Biochemistry Training Grant T01-GM-1046.[22] A.S. is an Alfred P. Sloan Fellow.

Appendix

Given the spectral density (eq 3), the calculation of T_1 and NOE are obtained directly from the expressions given in Table I of ref 1 for the case of heteronuclear ($I \neq S$) dipolar relaxation. In the calculations presented above, the ^{13}C–^1H bond length, r, has been taken as 1.09 Å. This value has been called into question for C^α–H bond lengths,[21] but for the C^α calculations presented here, changing this bond length by as much as ±0.02 Å has little effect.

(18) Wittebort, R. J. Ph.D. Thesis, Indiana University, 1978.

(19) Glushko, V.; Lawson, P. J.; Gurd, F. R. N. *J. Biol. Chem.* **1972**, *247*, 3176.

(20) Wittebort, R. J.; Rothbgeb, T. M.; Szabo, A.; Gurd, F. R. N. *Proc. Natl. Acad. Sci. U.S.A.* **1979**, *76*, 1059.

(21) Dill, K.; Allerhand, A. *J. Chem. Soc.* **1979**, *10*, 4376.

(22) This is the 121st paper in a series dealing with coordination complexes and catalytic properties of proteins and related substances.

For the free diffusion model the explicit expressions for $\lambda_{a,b,...}$ and $C_{a,b,...}$ used in $J'(\omega)$, eq 3, are for the ith carbon ($i = \beta, \gamma, \delta, \epsilon$).

$$\lambda_{b_1 b_2 \ldots b_i} = b_1^2 D_\beta + b_2^2 D_\gamma + \ldots + b_i^2 D_i \quad \text{(A1a)}$$

$$C_{b_1 b_2 \ldots b_i} = (d^{(2)}_{b_1 b_2}(\beta_{12}))^2 (d^{(2)}_{b_2 b_3}(\beta_{23}))^2 \ldots (d^{(2)}_{b_\beta}(\beta_{iF}))^2 \quad \text{(A1b)}$$

The functions $d^{(2)}_{ab}(\beta)$ are elements of the reduced Wigner rotation matrices, b_i are summation indexes taking on values from -2 to $+2$, $\beta_{i-1,i}$ are the angles between successive internal rotation axes, all 70.5°, and β_{iF} is the angle between the ith rotation axis and the C^i–H bond, also 70.5°.

The corresponding expressions for the restricted diffusion model are somewhat more complicated and thus each is given separately. For C^β

$$\lambda_{n_1} = n_1^2 \pi^2 D_\beta / 4\gamma_\beta^2 \quad \text{(A2a)}$$

$$C_{b_1 n_1} = \tilde{\Gamma}_{b_1 b_1 n_1}(\gamma_\beta)(d^{(2)}_{b_1 0}(\beta_{1F}))^2 \quad \text{(A2b)}$$

For C^γ

$$\lambda_{n_1 n_2} = \lambda_{n_1} + n_2^2 \pi^2 D_\gamma / 4\gamma_\gamma^2 \quad \text{(A3a)}$$

$$C_{b_1 b_2 b_2' n_1 n 2} = \tilde{\Gamma}_{b_1 b_1 n_1}(\gamma_\beta) d^{(2)}_{b_1 b_2}(\beta_{12}) d^{(2)}_{b_1 b_2'}(\beta_{12}) \tilde{\Gamma}_{b_2 b 2' n_2}(\gamma_\gamma) \times \cos[(b_2 - b_2')\alpha_{2F}] d^{(2)}_{b_2 0}(\beta_{2F}) d^{(2)}_{b_2' 0}(\beta_{2F}) \quad \text{(A3b)}$$

For C^δ

$$\lambda_{n_1 n_2 n_3} = \lambda_{n_1 n_2} + n_3^2 \pi_2 D_\delta / 4\gamma_\delta^2 \quad \text{(A4a)}$$

$$C_{b_1 b_2 b_2' b_3 n_1 n_2 n_3} = \tilde{\Gamma}_{b_1 b_1 n_1}(\gamma_\beta) d^{(2)}_{b_1 b_2}(\beta_{12}) d^{(2)}_{b_1 b_2'}(\beta_{12}) \tilde{\Gamma}_{b_2 b_2' n_2}(\gamma_\gamma) \times \cos[(b_2 - b_2')\alpha_{23}] d^{(2)}_{b_2 b_3}(\beta_{23}) d^{(2)}_{b_2' b_3}(\beta_{23}) \tilde{\Gamma}_{b_3 b_3 n_3}(\gamma_\delta) (d^{(2)}_{b_3 0}(\beta_{3F}))^2 \quad \text{(A4b)}$$

For C^ϵ

$$\lambda_{n_1 n_2 n_3 b_4} = \lambda_{n_1 n_2 n_3} + b_4^2 D_\epsilon \quad \text{(A5a)}$$

$$C_{b_1 b_2 b_2' b_3 b_4 n_1 n_2 n_3} = \tilde{\Gamma}_{b_1 b_1 n_1}(\gamma_\beta) d^{(2)}_{b_1 b_2}(\beta_{12}) d^{(2)}_{b_1 b_2'}(\beta_{12}) \tilde{\Gamma}_{b_2 b_2' n_2}(\gamma_\gamma) \times \cos[(b_2 - b_2')\alpha_{23}] \times d^{(2)}_{b_2 b_3}(\beta_{23}) d^{(2)}_{b_2' b_3}(\beta_{23}) \tilde{\Gamma}_{b_3 b_3 n_3}(\gamma_\delta) (d^{(2)}_{b_3 b_4}(\beta_{34}))^2 (d^{(2)}_{b_4 0}(\beta_{4F}))^2 \quad \text{(A5b)}$$

The β angles and b_i summation indexes are as in the free diffusion model, eq A1a and A1b. The functions $\tilde{\Gamma}_{bb'n}(\gamma)$ are given in ref 1, eq 3.12b and 3.12c, and the summation indexes used in this study, n_i, can be accurately truncated at $0 \le n_i \le 5$ for the amplitudes, γ, used in this study. The angles α_{2F} and α_{23} specify the torsional angles between the C^α–C^β bond and the C^γ–H or C^γ–C^δ bonds, respectively, when viewed along the C^β–C^γ bond with $\gamma_\gamma = 0$. For fluctuations about a trans C^α–C^δ–C^γ–C^δ configuration, $\alpha_{2F} = \pm 120°$ and $\alpha_{23} = 180°$. As one proceeds away from the "stationary" C^α end of the side chain, the torsional angle becomes meaningless if the internal rotations are assumed to be independent. Consequently the torsional angles specifying the angle between the C^δ–C^γ and C^δ–H or C^δ–C^ϵ bonds, α_{3F} and α_{34}, are averaged and do not appear. The angles α_{12} and α_{4F} rigorously do not appear since the motion of C^α is isotropic and that of C^ϵ is unrestricted.

An Electrode Modified with Polymer-Bound Dopamine Which Catalyzes NADH Oxidation

Chantal Degrand*[1a] and Larry L. Miller*[1b]

Contribution from the Laboratoire de Polarographie associe au CNRS, Faculte des Sciences Gabriel, 21000 Dijon, France, and the Department of Chemistry, University of Minnesota, Minneapolis, Minnesota 55455. *Received March 28, 1980*

Abstract: Dopamine was reacted with poly(methacryloyl chloride) producing a modified polymer with hydroquinone functionalities. The loading was 41%. This polymer was dip coated onto a vitreous carbon electrode from pyridine solution. Cyclic voltammetry was performed by using this electrode in buffered 0.1 M aqueous sodium chloride. The hydroquinone moieties could be oxidized to bound quinones in a chemically reversible process. Electrodes with varying amounts of polymer were prepared by varying the concentration of the solution from which the electrode was coated. The current integral indicated that these electrodes held from 0.05 to 0.75 nmol cm^{-2} of electroactive quinone functions. The pH dependence was studied and it was indicated that the hydroquinone moieties had a first p$K_a \approx 6$. The charging rate was shown to be relatively independent of pH, but dependent on the amount of polymer adsorbed. This modified electrode was used to catalyze the oxidation of NADH. The catalytic efficiency was measured and was shown to conform to stoichiometric expectations. It was demonstrated that the catalytic efficiency increased as the amount of electroactive polymer was increased from 0.05 to 0.2 nmol cm^{-2} but decreased for electrodes holding more polymer.

There is currently great interest in chemically modified electrodes. Of particular importance in the present context are experiments in which electroactive, molecular species, bound to the surface of conductors, are charged and in turn perform redox reactions on solution species.[2-7] This unusual form of electrocatalysis would seem to have applicability in several fields and the phenomenon raises a number of new, fundamental questions which have not been answered.

In the present work we hoped to provide answers to some of these questions. Particular attention was given to electrodes whose surfaces were coated with polymers[2b,4-6,8-16] and to pH-dependent

(1) (a) Laboratoire de Polarographie associe au CNRS. (b) University of Minnesota.
(2) (a) Evans, J. F.; Kuwana, T.; Henne, M. T.; Royer, G. P. *J. Electroanal. Chem.* **1977**, *80*, 409. (b) Van De Mark, M. R.; Miller, L. L. *J. Am. Chem. Soc.* **1978**, *100*, 3223.
(3) Tse, D. C. S.; Kuwana, T. *Anal. Chem.* **1978**, *50*, 1315.
(4) Kerr, J. B.; Miller, L. L. *J. Electroanal. Chem.* **1979**, *101*, 263.
(5) For photoinduced examples see: Bolts, J. M.; Wrighton, M. S. *J. Am. Chem. Soc.* **1979**, *101*, 6179. Bocarsly, A. B.; Walton, E. G.; Bradley, M. G.; Wrighton, M. S. *J. Electroanal. Chem.* **1979**, *100*, 283. Bolts, J. M., et al. *J. Am. Chem. Soc.* **1979**, *101*, 1378.
(6) Evans, J. F.; Dautartas, M. F. *J. Electroanal. Chem.*, in press. Evans, J. F., communication.
(7) Kobayashi, N.; Matsue, T.; Fujihira, M.; Osa, T. *J. Electroanal. Chem.* **1979**, *103*, 427.
(8) Kaufman, F. B.; Schroeder, A. H.; Engler, E. M.; Patel, V. V. *J. Am. Chem. Soc.* **1980**, *102*, 483.
(9) Miller, L. L.; Van De Mark, M. R. *J. Am. Chem. Soc.* **1978**, *100*, 639.
(10) Kaufman, F. B.; Engler, E. M. *J. Am. Chem. Soc.* **1979**, *101*, 547.
(11) Doblhofer, K.; Nolte, D.; Ulstrup, J. *Ber. Bunsenges. Phys. Chem.* **1978**, *82*, 403.
(12) Merz, A.; Bard, A. J. *J. Am. Chem. Soc.* **1978**, *100*, 3222.

0002-7863/80/1502-5728$01.00/0 © 1980 American Chemical Society